Enhanced donor heart preservation by therapeutic inhibition of acid sensing ion channel 1a

Meredith A. Redd[1,9†], Sarah E. Scheuer[2,3,4†], Natalie J. Saez[1], Ling Gao[2], Mark Hicks[2,4,5], Jeanette E. Villanueva[2,4], Melissa E. Reichelt[6], Jason N. Peart[7], Louise E. See Hoe[8,9], Han S. Chiu[1], Xiaoli Chen[1], Yuliangzi Sun[1], Jacky Y. Suen[8,9], Robert J. Hatch[10], Ben Rollo[10], Mubarak A.H. Alzubaidi[1], Snezana Maljevic[10], Gregory A. Quaife-Ryan[11], Walter G. Thomas[6], James E. Hudson[11], Enzo R. Porrello[12,13], Gabriel Cuellar-Partida[14], John F. Fraser[8,9], Steven Petrou[10], Glenn F. King[1]*, Peter S. Macdonald[2,3,4]* & Nathan J. Palpant[1]*

[1]Institute for Molecular Bioscience, The University of Queensland, St. Lucia, Australia.

[2]Victor Chang Cardiac Research Institute, Sydney, Australia.

[3]Cardiopulmonary Transplant Unit, St. Vincent's Hospital, Sydney, Australia.

[4]Faculty of Medicine, University of New South Wales, Sydney, Australia.

[5]Department of Pharmacology, St. Vincent's Hospital, Sydney, Australia.

[6]School of Biomedical Sciences, The University of Queensland, St. Lucia, Australia.

[7]School of Medical Science, Griffith University, Southport, Australia.

[8]Faculty of Medicine, The University of Queensland, Brisbane, Australia.

[9]Critical Care Research Group, The Prince Charles Hospital and The University of Queensland, Brisbane, Australia.

[10]Florey Institute of Neuroscience and Mental Health, The University of Melbourne, Melbourne, Australia.

[11]QIMR Berghofer Medical Research Institute, Brisbane, Australia.

[12]Murdoch Children's Research Institute, The Royal Children's Hospital, Melbourne, Australia.

[13]Department of Physiology, School of Biomedical Sciences, The University of Melbourne, Parkville, Australia.

[14]The University of Queensland Diamantina Institute, Faculty of Medicine and Translational Research Institute, Woolloongabba, Australia.

†These authors contributed equally.

*Corresponding authors: Nathan J. Palpant, Glenn F. King, and Peter S. Macdonald

Email: n.palpant@imb.uq.edu (N.J.P), glenn.king@imb.uq.edu.au (G.F.K), peter.macdonald@svha.org.au (P.S.M)

Classification: Biological Sciences/Medical Sciences

Keywords: ASIC1a, ischemia reperfusion injury, heart transplant, cardioprotection

Abstract

Ischemia reperfusion injury (IRI) is one of the major risk factors associated with primary graft dysfunction, the leading cause of early mortality in heart transplant recipients. Here, we show that the proton-gated acid-sensing ion channel 1a (ASIC1a) plays a key role during cardiac ischemia and demonstrate that ASIC1a is a promising new target to improve the tolerance of cardiac tissue to IRI. Genetic ablation of ASIC1a leads to improved functional recovery following global myocardial IRI in *ex vivo* mouse hearts, and this effect can be recapitulated by therapeutic blockade of ASIC1a using specific and potent venom-derived pharmacological inhibitors. Using two models of donor heart procurement and storage, we show that ASIC1a inhibition yields improved post-IRI cardiac viability and function as a pre- or post-conditioning agent, with organ recovery equal to benchmark drugs including the sodium-hydrogen exchange inhibitor, zoniporide. Using human pluripotent stem cells, we show that ASIC1a inhibition improves cardiomyocyte viability under conditions of acidosis or ischemia *in vitro*. At the cellular and whole organ level, we show that acute exposure to ASIC1a inhibitors have no impact on cardiac electromechanical coupling and physiological performance. Consistent with a key role for ASIC1a in human cardiac ischemia, we used summary data from GWAS to show that polymorphisms in the ASIC1 genetic locus are strongly associated with susceptibility to cardiac ischemic injuries. Collectively, our data provide compelling evidence for a novel pharmacological strategy involving ASIC1a blockade as a cardioprotective therapy to improve the viability of donor hearts exposed to myocardial ischemia.

Significance Statement

Ischemia-reperfusion injury (IRI) is the primary reason for early allograft failure after heart transplantation. IRI is also implicated in the pathophysiology of diverse post-ischemic heart diseases that are a leading cause of morbidity and mortality worldwide. There are currently no drugs available to protect the heart from IRI. This study uses genetic approaches to demonstrate a novel role for ASIC1a in mediating the response of the heart to IRI. In addition, we identify venom-derived ASIC1a inhibitors as novel pharmacological therapeutics for cardiovascular medicine, in particular for the preservation of donor hearts destined for transplantation.

Introduction

Heart transplantation remains the most effective treatment option for patients with heart failure (HF), a disease that affects over 26 million people worldwide (1, 2). It is estimated that 1 in 5 people develop heart failure, with an annual healthcare cost of $108B (3, 4). Despite the effectiveness of heart transplantation, 75% of potential donor hearts are discarded, many due to donor heart sensitivity to ischemic injury (2). Even in successfully transplanted hearts, primary graft dysfunction is a major risk for patients in the first 30 days after transplantation, and it accounts for 66% of patient deaths, of which 48% are due to ischemia-reperfusion injury (IRI) (5). Furthermore, the relative risk of one-year morbidity following transplantation is strongly correlated with organ ischemic time (2, 6). Myocardial sensitivity to IRI therefore remains a primary point of vulnerability underlying the number of available donor hearts and patient outcomes.

Myocardial IRI is a complex pathophysiological process that underlies the cardiac injury sustained during donor organ procurement, storage, and transplantation. During ischemia, reduced oxygen availability causes a shift from fatty acid metabolism to anaerobic glycolysis (7, 8). The resulting lactic acidosis causes the extracellular pH to fall to as low as 6.0–6.5 (9, 10). Ongoing acidosis results in the activation of several transmembrane ion channels and receptors, including the sodium-hydrogen exchanger (NHE), glutamate-gated NMDA receptors, and the TRP family of ion channels, each of which are thought to contribute to calcium overload, metabolic dysfunction, and eventually cell death (11-13).

Acid sensing ion channels (ASICs) are voltage-independent, proton-gated cation channels of the degenerin/epithelial sodium channel superfamily (14). There are six ASIC isoforms derived from four genes (*ACCN1–4*), which assemble into homotrimeric or heterotrimeric channels. The pH sensitivity and kinetics of ASICs are determined by their subunit composition (15, 16). ASICs are involved in extracellular acidification-induced calcium overload in neurons and cardiomyocytes (17-19). ASIC1a, a splice variant of the *ACCN1* gene, is the most pH-sensitive ASIC channel. Activation begins at pH ≤ 7, with half-maximal activation at pH 6.6 (20, 21), and ASIC1a currents are potentiated by numerous metabolic events that occur during ischemia including membrane stretch and increased levels of extracellular lactate, pyruvate, and arachidonic acid (22, 23). ASIC1a plays a critical role in mediating ischemia-induced neuronal death, and inhibition of ASIC1a through genetic ablation or pharmacological blockade is neuroprotective in rodent models of ischemic stroke (24-27). ASIC1a has not been studied in the context of cardiac ischemia and its role in the heart is largely unknown.

In this study, we used genetic and pharmacological approaches to demonstrate that ASIC1a is a critical mediator of the injury response to myocardial IRI. We show that venom-derived inhibitors

3

of ASIC1a provide robust cardioprotection across multiple species and model systems from the cellular to whole-organ level. We demonstrate a reproducible benefit in organ recovery using multiple models of donor heart preservation and provide compelling evidence that ASIC1a is an important target for cardioprotective drugs, with potential clinical application in whole heart transplantation.

Results

Genetic ablation of ASIC1a improves functional recovery following cardiac IRI. We assessed ASIC isoform expression in the adult mouse heart using transcriptomic data of sorted cardiac cell populations (28). *ASIC1* expression was highest in cardiomyocytes, while endothelial cells and fibroblasts expressed both *ASIC1* and *ASIC3*. In all three cell types, *ASIC4* and *ASIC2* had low and undetectable expression, respectively (**Fig. 1A**). *ASIC1* encodes two isoforms from the same genetic locus, ASIC1a and ASIC1b, that are genetically conserved in bilaterians. As opposed to ASIC1b, which is primarily involved in nociception (29), we focused on ASIC1a due to its known role in mediating ischemic injury in the brain (16).

To determine whether ASIC1a plays a functional role during cardiac ischemia, we assessed IRI tolerance of Langendorff-perfused isolated hearts from ASIC1a-specific knockout (KO) mice. To generate the ASIC1a KO mouse strain, we used CRISPR editing to target the *ACCN1* locus. Specificity of the knockout was confirmed using qRT-PCR which showed that *ASIC1a* but not *ASIC1b* mRNA was reduced in brain tissue from knockout (KO) mice (**Supplemental Fig. S1**). Baseline function and heart rate in ASIC1a KO (ASIC1a$^{-/-}$) isolated hearts were comparable to those measured in wild-type (WT) control hearts (ASIC1a$^{+/+}$) (**Table 1**). To assess tolerance to IRI, hearts were subjected to 25 min of global normothermic zero-flow ischemia, followed by 45 min of aerobic reperfusion. WT and ASIC1a KO hearts showed similar initial responses to ischemia with comparable levels of ventricular contracture (**Supplemental Fig. S2A**). During reperfusion, both groups demonstrated gradual recovery of contractile function over time, with markedly improved functional recovery in ASIC1a KO hearts (**Fig. 1B**). By the end of the reperfusion period, ASIC1a KO hearts had significantly improved systolic and diastolic function with higher left ventricular developed pressure (LVDP) (44 $\pm$ 5% of baseline) and lower end diastolic pressure (EDP) (38 $\pm$ 3 mmHg) compared to WT hearts (LVDP: 23 $\pm$ 7% of baseline; EDP: 50 $\pm$ 3 mmHg; **Fig. 1 C** and **D**). ASIC1a KO hearts also had improved recovery of coronary flow (CF) rates by the end of reperfusion (KO: 97 $\pm$ 6%; WT: 78 $\pm$ 3%, percent baseline) (**Fig. 1E** and **Supplemental Fig. S2 B** and **C**). To assess cell death, lactate dehydrogenase (LDH) efflux was measured in perfusate samples collected during reperfusion. LDH efflux from ASIC1a KO hearts was significantly lower compared to WT hearts after 2 min of

4

reperfusion (**Fig. 1F**), with a similar trend at the end of reperfusion (**Supplemental Fig. S2D**). Our data indicate that ASIC1a does not play a role in maintaining functional homeostasis, but it is a critical mediator of the organ response to myocardial IRI.

ASIC1a inhibitors protect mouse hearts against IRI. We sought to determine whether pharmacological inhibition of ASIC1a is similarly cardioprotective to genetic ablation of the channel. Despite significant investment and preclinical testing, drug development pipelines have failed to identify effective small-molecule inhibitors of ASIC1a due to lack of specificity, potency, or functional efficacy (30-32). We therefore took advantage of two venom-derived inhibitors of ASIC1a, both of which are highly selective for ASIC1a, with no effect on other ASIC isoforms (24, 26). Hi1a is a 76-residue double-knot peptide isolated from the venom of an Australian funnel-web spider (**Fig. 2A**); it is the most potent and selective inhibitor of ASIC1a identified to date, with an IC_{50} on rat and human ASIC1a of ~500 pM (26). PcTx1, a single-knot peptide from the venom of a tarantula, is also a potent and selective inhibitor of ASIC1a (IC_{50} ~1 nM) (24). Although the two peptides are closely related (Hi1a is comprised of two PcTx1-like domains joined by a short linker; **Fig. 2 B** and **C**), they have distinct inhibitory modes of action. Hi1a inhibits ASIC1a activation whereas PcTx1 promotes and stabilizes a desensitized state of the channel (26). We also utilized an analogue of PcTx1 that contains mutations of two pharmacophore residues (R27A/V32A), which dramatically reduces its inhibitory effect on ASIC1a (24).

To examine if these ASIC1a inhibitors are cardioprotective, we assessed tolerance to IRI in Langendorff-perfused isolated mouse hearts with and without peptide treatment. Consistent with genetic ablation of ASIC1a, Hi1a, PcTx1, and PcTx1-R27A/V32A had no effect on baseline contractile function during the first 10 min of peptide infusion prior to ischemia (**Fig. 2D**). Functional tolerance to IRI was greater in hearts exposed to Hi1a or PcTx1 (10 nM) compared to control hearts (**Fig. 2E**). At the end of reperfusion, Hi1a- and PcTx1-treated hearts, but not hearts treated with the functionally impaired PcTx1-R27A/V32A analogue, had markedly improved recovery of LVDP (Hi1a: $60 \pm 4\%$, PcTx1: $49 \pm 12\%$, PcTx1-R27A/V32A: $36 \pm 6\%$) compared to vehicle controls ($20 \pm 4\%$) (**Fig. 2F**). Similarly, treatment with Hi1a and PcTx1, but not PcTx1-R27A/V32A, led to reduced EDP after 45 min reperfusion (Hi1a: 35 ± 4 mmHg; PcTx1: 33 ± 8 mmHg; PcTx1-R27A/V32A: 48 ± 3 mmHg) compared to vehicle controls (57 ± 2 mmHg) (**Fig. 2G**). No differences in final CF were observed between groups (**Fig. 2H**), although hearts treated with PcTx1, but not Hi1a, displayed significant reactive hyperaemia during early reperfusion, as evidenced by increased CF during the first 5 min of reperfusion (**Supplemental Fig. S3 A** and **B**). Taken together, our data show that ASIC1a inhibitors protect the heart from myocardial IRI and recapitulate the functional benefits of genetic

5

ablation of the channel.

Preconditioning with Hi1a improves functional recovery of isolated rodent hearts after prolonged hypothermic ischemia. In order to evaluate the cardioprotective effect of ASIC1a inhibition in a model of donor heart preservation, we supplemented standard clinical heart preservation solution (Celsior (33)) with Hi1a during 8 h cold storage of isolated rat hearts. The hearts were stabilised for 10 min by retrograde (Langendorff) perfusion and then switched to working-mode in order to assess cardiac function in the presence of physiological afterload. Following assessment of baseline hemodynamic parameters, hearts were arrested by infusion of cold (2–3°C) Celsior solution with and without 10 nM Hi1a into the coronary circulation. After cardioplegic arrest, hearts were stored under hypothermic conditions for 8 h, followed by reperfusion and functional analysis (**Fig. 3A**). Hearts preserved with Hi1a supplementation had markedly improved recovery of aortic flow (AF) ($50 \pm 11\%$) and cardiac output (CO) ($57 \pm 8\%$) compared to Celsior-only controls (AF: $8 \pm 5\%$; CO: $24 \pm 5\%$) (**Fig. 3 B** and **C**). These data demonstrate that Hi1a is highly cardioprotective against IRI in a clinically relevant model of donor heart preservation with prolonged cold storage.

Hi1a supplementation improves recovery in a post-conditioning model of donation after circulatory death. To determine whether pharmacological inhibition of ASIC1a could recover hearts when delivered subsequent to a profound ischemic injury, we assessed the effect of Hi1a in a rodent model of donation after circulatory death (DCD). To mimic a clinical DCD withdrawal for heart transplantation in rodents, asphyxiation was induced via tracheal ligation, then the hearts were retrieved after a 10-min warm ischemic time (WIT) followed by 2-min stand-off period. Following ischemia, the hearts were flushed with Celsior with or without supplementation, followed by *ex vivo* reperfusion in Langendorff mode for 30 min and then working mode for an additional 30 min (**Fig. 4A**).

Hi1a (10 nM) was tested as a single supplement and in combination with two clinically used supplements, glyceryl trinitrate (GTN) and erythropoietin (EPO) (34). As a positive control, we also evaluated zoniporide (Zon) combined with GTN and EPO, which we have previously shown activates ischemic postconditioning pathways through inhibition of NHE activity (35). To assess the viability of hearts post-DCD withdrawal, functional parameters and cell death (LDH release) were measured throughout working-mode reperfusion. In Celsior-only controls, coronary effluent levels of LDH increased throughout the 30 min assessment period. Allografts supplemented with Hi1a, Hi1a + GTN/EPO, or GTN/EPO/Zon, however, had significantly reduced levels of LDH after 30 min, with

6

LDH release in both triple-supplemented groups comparable to a heart at baseline, prior to ischemic insult (**Fig. 4B**). Functional parameters of recovery including AF, CO, and pulse pressure (PP) were all significantly improved in supplemented groups compared to Celsior alone (**Fig. 4 C–E**). AF, in particular, was significantly increased in hearts supplemented with Hi1a combined with GTN and EPO (32 ± 2 mL/min) compared to Hi1a as a single supplement (18 ± 3 mL/min), suggesting an additive effect of Hi1a with current clinically used cardioprotective agents (**Fig. 4C**).

To investigate the therapeutic benefit of Hi1a in the context of preventing cell death in DCD hearts, we performed western blots to examine the levels of phosphorylated RIP3 (pRIP3) in tissue lysates collected at the end of working-mode reperfusion. RIP3 is one of the key regulators of the necroptosis pathway that has been implicated in the response to IRI (36, 37), and specifically to ASIC1a-mediated cell death during cerebral ischemia (38). Treatment with Hi1a as a single or triple supplement led to reduced levels of pRIP3 following DCD withdrawal and reperfusion (**Fig. 4F**), suggesting that Hi1a blockade of ASIC1a might inhibit necroptosis. Together with our finding that Hi1a improved donor organ viability after prolonged cold storage, the therapeutic efficacy of Hi1a in the DCD model demonstrates significant translational potential for ASIC1a-targeted therapies during clinical donor heart preservation.

ASIC1 is expressed in the human heart and polymorphisms in its genetic locus are associated with ischemic disease. Analysis of ASIC expression patterns from mRNA-seq and ribo-seq data collected from human left ventricular cardiac tissue (39) revealed the highest expression of *ASIC1* and *ASIC3* in the human left ventricle and similar levels of *ASIC1* expression in samples from HF and non-HF patients (**Supplemental Fig. S4 A** and **B**).

We next assessed whether natural variation in the genetic locus encoding ASIC1a (*ACCN1*) is associated with ischemic diseases using human population statistical genetics. While fewer than 10% of new molecular entities that pass through clinical trials are approved for therapeutic use, evidence of human genetic association between the gene target and traits sufficiently similar to the indication being treated increases the likelihood of approval to as high as 50% (40). We utilized summary data from genome-wide association studies (GWAS) (41) and calculated the statistical significance (using fastBAT (42)) of genetic variants encompassing the *ACCN1* locus with human cardiac and cerebral ischemic phenotypes. These data revealed a significant association between genetic variation in *ACCN1* and major coronary heart disease and MI ($P < 0.05$) (**Table 2**). We also found that genetic variation in *ACCN1* associates with small-vessel ischemic stroke ($p = 3.94 \times 10^{-3}$), but not other stroke subtypes (**Table 2**). Taken together, these data provide evidence that *ACCN1* polymorphisms within the human population are associated with ischemic diseases of the heart and brain.

ASIC1a inhibition prevents cell death in in vitro human models of IRI. To examine whether pharmacological blockade of ASIC1a might provide therapeutic benefit in the context of human tissue, we used human induced pluripotent stem cell-derived cardiomyocytes (hiPSC-CMs). Contractile cardiomyocytes were generated from stem cells using a standard monolayer-based differentiation protocol involving bi-phasic Wnt regulation (**Fig. 5A** and **Supplemental Fig. S5A**). Analysis of mRNA transcripts from single-cell RNA sequencing data over a time course of cardiac differentiation from pluripotency (43) revealed that *ASIC1*, *ASIC3*, and *ASIC4* expression increased starting in day-5 cardiac progenitor populations and peaked in day-15 definitive cardiomyocytes. *ASIC1* was the most highly expressed ASIC subtype, with expression levels comparable to other cardiac ion channels such as TRPV1 and Nav1.5 (**Fig. 5 B** and **C**).

Since ASIC1a mediates influx of calcium in addition to sodium (29), we performed calcium imaging after acute addition of the ASIC1a inhibitors Hi1a and PcTx1 to assess whether ASIC1a inhibition alters physiological electromechanical coupling in cardiomyocytes. Replated hiPSC-CMs were loaded with a fluorescent calcium dye and calcium transients were recorded before and after peptide addition. Neither Hi1a nor PcTx1 altered calcium amplitudes or spontaneous beating rate at any evaluated concentration (**Fig. 5D**).

To assess whether ASIC1a inhibition is cardioprotective in hiPSC-CMs, we evaluated cell death in response to *in vitro* acidosis, induced by culturing hiPSC-CMs in Hank's buffered sodium salt (HBSS) with pH adjusted to pH 7.4, 6.0, or 5.0. *ASIC1* mRNA expression was not significantly altered by low pH treatment, but significant cell death (> 40%), as assessed by LDH secretion, was observed in cultures treated overnight at pH 5.0, with minimal cell death occurring at pH 7.4 or pH 6.0 (**Supplemental Fig. S5 B** and **C**). Treatment with either Hi1a or PcTx1 resulted in nearly complete cardioprotection, even at concentrations as low as 1 nM (**Fig. 5E** and **Supplemental Fig. S5 D** and **E**). To further confirm that ASIC1a plays a direct role in mediating cell death, we treated hiPSC-CMs overnight with 20 nM MitTx, a potent agonist of ASIC1a isolated from snake venom (44). Consistent with ASIC1a mediating the injury response to cardiac ischemia, treatment of hiPSC-CMs with MitTx resulted in increased cell death at both pH 7.4 and pH 6.0 (**Fig. 5F**).

We next evaluated the cardioprotective effect of Hi1a and PcTx1 in an *in vitro* model of ischemia/acidosis with reperfusion. To mimic ischemia/acidosis *in vitro*, hiPSC-CMs were incubated overnight under combined hypoxic (0.5% O_2) and acidic (pH 5.0) conditions with or without peptide. After 18 h of incubation, the low-pH medium was replaced with medium at physiological pH 7.4 with or without peptide, and the cells were incubated for an additional hour under normoxic conditions. Significant cell death was observed in control hiPSC-CMs, but this was blocked by either 10 nM Hi1a or PcTx1 (**Fig. 5 G** and **H**). These data suggest that ASIC1a mediates cell death responses in human

cardiomyocytes and that pharmacological inhibition of ASIC1a confers significant protection against ischemia-induced cell stress.

Discussion

In this study, we showed that ASIC1a exacerbates cardiomyocyte injury responses to ischemia, and that inhibition of ASIC1a during IRI affords significant cardioprotection. Although ASICs, and in particular ASIC1a, are generally associated with the central and peripheral nervous systems (45), our expression analyses revealed that ASIC1 is present in both rodent and human cardiomyocytes, and is not differentially regulated at the transcriptional level as a result of cellular ischemia *in vitro*. Our evidence of ASIC1 expression in the heart is supported by recent studies that identified ASIC-like currents in hiPSC-CMs (46) and rat cardiomyocytes (17). In neurons, there are several possible mechanisms by which ASIC1a activation leads to cell death including calcium overload (47), regulation of mitochondrial permeability transition (MPT) pores (48), and the initiation of necroptosis through direct interaction with, and activation of, RIPK1 (38). ASIC1a-induced cell death has not previously been described in cardiomyocytes, but there is evidence that ASIC1a, along with TRPV1, mediates calcium influx in response to extracellular acidosis (17). Importantly, given the potential for ASIC1a to transport calcium, we showed that genetic ablation or pharmacological inhibition of ASIC1a does not alter normal electromechanical coupling in the heart *in vitro* or *in vivo*.

Our finding that ASIC1a blockade protects the heart from IRI-associated cardiac dysfunction is consistent with prior research demonstrating the importance of ASIC1a during cerebral ischemia (24-27), and it extends the potential therapeutic applications of ASIC1a-targeted therapies to cardiac applications, such as the preservation of donor hearts for transplantation. The majority of heart transplants are performed with hearts donated from brain dead (BD) donors, as hearts from the DCD pathway were historically considered unusable for transplantation due to the severe ischemic injury sustained during organ procurement (49). Recent advances, however, have shown that successful transplantation of DCD hearts is possible with effective post-conditioning strategies, namely normothermic *ex vivo* perfusion and pharmacological post-conditioning. There are now active DCD transplant programmes in Australia and Europe, as well as a large multi-centre trial in the USA (34, 35, 50). The viability of usable BD and DCD hearts, however, continues to be adversely affected by unavoidable injury to the heart that occurs during organ procurement and storage, as well as reperfusion injury in the recipient. The development of early interventions that reduce injury to the graft and reduce the risk of primary graft dysfunction in the recipient therefore remains a critical area of research and unmet need.

NHE inhibitors showed promise as an intervention for improving ischemic tolerance of DCD hearts (35, 51), as well as in a number of other clinical indications of myocardial IRI including cardiac surgery (52). However, in a Phase III clinical trial (the EXPEDITION Trial) of the NHE inhibitor cardiporide, cerebrovascular complications halted therapeutic development, despite promising clinical evidence that NHE inhibitors can be effective at reducing myocardial IRI (53). Our direct comparison between Hi1a and current clinical preservation supplements as well as the NHE inhibitor, zoniporide, provide strong evidence for the clinical utility of ASIC1a inhibitors.

Given that drug targets with genetic evidence of disease association are twice as likely to succeed in clinical trials and lead to approved drug candidates (40), our GWAS analysis of the association between genetic variation in the *ACCN1* locus and ischemic disease points towards the translational potential of ASIC1a-targeted therapies. Such therapies have the potential to impact a broad scope of clinical applications since myocardial IRI is evident in many cardiovascular complications outside of heart transplantation, such as acute MI, out-of-hospital cardiac arrest (OHCA), and cardiopulmonary bypass surgery (2). Despite intensive research into therapies aimed at mitigating myocardial IRI in the context of acute MI, none have translated into clinical practice (54). Furthermore, ASIC1a inhibitors might provide a potential major advantage for clinical use due to their ability to protect both the heart and the brain from IRI, which is particularly relevant for OHCA that results in cardiac and cerebral ischemia. In general, there is a strong association and co-morbidity between stroke and cardiac arrest, with 88% of patients suffering some form of cardiovascular complication within four weeks of an ischemic stroke (55). Likewise, cardiac interventions such as transcatheter aortic valve implantation (TAVI) can cause cerebrovascular complications (56). We previously used a rat model of ischemic stroke to show that a single dose of Hi1a (2 ng/kg i.c.v) massively reduced infarct size and improved neurological and motor performance even when administered up to 8 h after stroke onset (26). No other drugs have been shown to provide significant protection beyond 4 h after stroke onset (57).

Venom-derived molecules have proven to be a source of novel therapeutics, particularly in the cardiovascular field. Examples include the antihypertensive drug captopril (58) derived from the venom of a Brazilian viper, and eptifibatide and tirofiban, antiplatelet drugs that are used to treat acute coronary syndromes (59). Disulfide-rich knottin peptides such as Hi1a are typically highly stable in biological fluids, and ziconitide, a knottin peptide derived from cone snail venom, is an FDA-approved analgesic (59). For this reason, Hi1a is ideally suited for clinical use as an adjuvant to standard-of-care heart preservation solutions for heart transplant or in combination with mechanical procedures such as percutaneous coronary intervention for myocardial infarction.

In summary, we have shown that ASIC1a is a critical mediator of cell death during cardiac

ischemia and that pharmacological inhibition of ASIC1a affords potent cardioprotection across rodent and human models of cardiac IRI. These findings suggest that ASIC1a inhibitors have the potential to significantly impact the public health burden of cardiovascular disease and result in improved outcomes for patients with cardiac ischemic injuries.

Materials and Methods

Study Design. All animal experiments were performed in accordance with protocols approved by the Animal Ethics Committee of The University of Queensland (IMB/171/18) and Garvan Institute of Medical Research (16/38). All hiPSC studies were performed with consent from The University of Queensland's Institutional Human Research Ethics approval (HREC 2015001434). Additional information for each set of experiments, such as statistical analyses, exclusion criteria, and sample size, are detailed in the relevant methods section or figure legend. All data and materials associated with this study can be provided upon request.

Animals. All animals used in this study received humane care in compliance with National Health and Medical Research Council (Australia) guidelines and the *Guide for the Care and Use of Laboratory Animals* (National Institute of Health, Bethesda, MD). To test the therapeutic efficacy of ASIC1a inhibitors, male C57BL/6 mice (Langendorff IRI experiments) or male Wistar rats (donor organ preservation experiments) were purchased from the Animal Resource Centre (Canning Vale, Western Australia).

For genetic ablation studies, ASIC1a$^{-/-}$ mice were generated at the Australian Phenomics Facility. CRISPR/Cas9 technology was used to specifically target the mouse ASIC1a sequence. Use of guide RNAs (gRNA) with the sequences CCGAGGAGGAGGAGGTGGGTGGT and GTACCATGCTGGGGAACTGCTGG resulted in single nucleotide deletions within both targeted regions, at positions 22 and 341 (NM_009597.2(ASIC1_v001):c.22del and NM_009597.2(ASIC1_v001):c.341del). These deletions predicted a disrupted ASIC1a protein sequence (p.Glu8Argfs*9 and p.Leu114Argfs*94, respectively). The founder mouse was backcrossed to C57BL/6 background. Both hetero- and homozygous mice were viable and showed no obvious phenotype. Total RNA was isolated from brain tissue using Trizol Reagent (ThermoFisher Scientific, Massachusetts, USA), and contaminant genomic DNA was removed with DNA-free reagents (Ambion/Life Technologies, Austin, USA). Primer sequences designed to distinguish between ASIC1a and ASIC1b transcripts were used to determine gene expression levels in ASIC1a KO and WT animals (60). Primers sequences used in this study were ASIC1a forward 5′-

11

CTGTACCATGCTGGGGAACT-3′ and reverse 5′-GCTGCTTTTCATCAGCCATC-3′; ASIC1b forward 5′-TGCCAGCCATGTCTTTGTG-3′ and reverse 5′-CACAGGAAGGCACCCAGT-3' and RPL32 (for sample normalization) forward 5'-GAGGTGCTGCTGATGTGC-3' and reverse 5'-GGCGTTGGGATTGGTGACT-3'. For quantitative real-time (qRT)-PCR, oligo-dT primed cDNA was synthesized from 500 ng of total RNA using Murine Moloney Leukaemia Virus reverse transcriptase (Promega, USA). qRT-PCR was performed using a ViiA Real-Time PCR System (Applied Biosystems, California, USA) using SYBR green master mix (Promega, USA) according to manufacturer protocols. Relative ASIC1a and ASIC1b gene expression values were obtained from ASIC1a$^{-/-}$ mice and WT (ASIC1a$^{+/+}$) mice (calibrator) by normalization to the reference gene RPL32 using the 2-$\Delta\Delta$Ct method, where 2-$\Delta\Delta$Ct = ΔCt sample – ΔCt calibrator.

IRI in Langendorff-perfused mouse hearts. Isolated hearts were assessed for tolerance to IRI as previously described (61, 62). Mice (12–14 weeks) were anesthetized via an intraperitoneal injection of 10 mg/mL ketamine and 1.6 mg/mL xylazil. The heart was excised via thoracotomy and the aorta was cannulated. The hearts were retrogradely perfused under constant hydrostatic pressure (80 mmHg) with oxygenated (95% O_2; 5% CO_2) modified Krebs-Henseleit buffer (composition in mM: 119 NaCl, 22 $NaHCO_3$, 4.7 KCl, 1.2 $MgCl_2$, 1.2 KH_2PO_4, 0.5 EDTA, 1.85 $CaCl_2$, 11 D-(+)-glucose, 2 Na$^+$ pyruvate, all from Sigma-Aldrich). Temperature was continuously measured with thermocouple needle microprobes (SDR Scientific) and maintained at 37°C with circulating water baths. Contractile function was measured via a fluid-filled balloon inserted in the left ventricle and connected to a pressure transducer (ADInstruments Pty Ltd.). Coronary flow was measured with an in-line Doppler flow probe positioned above the aortic cannulae (Transonic Systems Inc.). All functional data were recorded on a four-channel MacLab system (ADInstruments Pty Ltd.). Following 15–30 min of equilibration, hearts were switched to ventricular pacing at 420 beats/min (BPM) using a SD9 stimulator (Grass Instruments, Inc.). Baseline measurements were made for 10–20 min followed by 25 min of global normothermic ischemia and 45 min of reperfusion. Pacing was stopped during ischemia and resumed after 15 min of reperfusion. For peptide-treated experimental groups, 1 μM peptide solution was infused with a syringe pump (World Precision Instruments, LLC.) into the buffer, directly upstream of the cannula, at a rate of 1% of CF, for a final working concentration of 10 nM. Peptide was infused for 10 min prior to the onset of ischemia and during the first 15 min of reperfusion. To assess cell death, effluent was collected at 2 and 45 min after the start of reperfusion. Effluent levels of LDH were measured using a cytotoxicity detection kit (Roche). Normalized absorbance values (absorbance at 492 nm minus absorbance at 690 nm) were measured using a PHERAStar FS microplate reader (BMG Labtech). Standard curves were generated with bovine LDH (Sigma-Aldrich) and used

to convert sample absorbance values to units of LDH. Data were normalized to CF and heart weight and then expressed as U/min/g. For all analyses, hearts were excluded if they had abnormally high coronary flow (> 8 mL/min), delayed onset of ischemic contracture (time to onset of ischemic contracture (TOIC) > 20 min), poor contractile function after equilibration (significant arrhythmias and/or left ventricular systolic pressure < 80 mmHg), or technical issues with the perfusion rig.

Isolated working model of donor heart preservation after prolonged cold storage. The isolated working heart model of donor heart preservation has been previously described (63-65). Male Wister rats (325–395 g) were anesthetized with an intraperitoneal injection of ketamine (80 mg/kg; Cenvet, Australia) and xylazine (10 mg/kg; Provet, Australia), with supplemental doses given as necessary until adequate anaesthesia was achieved. An incision was made in the abdomen of the animal and a bolus injection of 300 IU of heparin administered into the renal vein. A sternotomy was performed and the heart was excised and arrested by immersion in ice-cold Krebs-Henseleit buffer (composition in mM: 118 NaCl, 4.7 KCl, 1.2 $MgSO_4$, 1.2 KH_2PO_4, 25 $NaHCO_3$, 1.4 $CaCl_2$, 11 glucose, all from Sigma-Aldrich). Following aortic cannulation, hearts were stabilised for 10 min by retrograde (Langendorff) perfusion with Krebs-Henseleit buffer (37°C), at a hydrostatic pressure of 100 cm H_2O. During this period, the left atrial appendage was cannulated. This nonworking Langendorff system was converted to a working preparation by switching the supply of perfusate from the aorta to the left atrial cannula at a hydrostatic pressure of 15 cm H_2O (preload). The working heart ejected perfusate into the aortic cannula against the maintained fixed hydrostatic pressure of 100 cm H_2O (afterload). Aortic pressure was monitored via a side arm of the aortic cannula with a pressure transducer (Ohmeda, Pty Ltd., Singapore). AF was measured by an in-line flowmeter (Transonics Instruments Inc., Ithaca, NY). Aortic pressure and flow were recorded using PowerLab/4e (ADInstruments Pty Ltd, Sydney, Australia) with heart rate (HR) calculated from the flow trace. CF was measured by timed collection of effluent draining from the heart via a small incision in the pulmonary artery (PA). CO was calculated from the sum of AF and CF. The hearts were maintained in working mode for 15 min, at which time functional parameters (AF, CF, CO and HR) were recorded and defined as the baseline value. Any hearts having a baseline AF < 35 mL/min, HR < 200 bpm, or CF < 10 mL/min were excluded at this stage. The heart was arrested by infusion of a preservation flush containing Celsior solution (2–3°C) ± 10 nM Hi1a via the aortic cannula (60 cm H_2O infusion pressure over 3 min), immersed in 100 mL Celsior ± 10 nM Hi1a, and kept on ice for 8 h. The heart was remounted on the perfusion apparatus and perfused with fresh Krebs-Henseleit buffer for 15 min in Langendorff mode, followed by 30 min in working mode. Celsior solution was obtained from the Institut Georges Lopez (Lissieu, France).

13

Cardiac functional indices after 30 min of working-mode reperfusion were expressed as percent recovery of baseline values.

Donor heart preservation following circulatory death in rodents. The rodent model of DCD (**Fig. 4A**) was developed by our laboratory to closely mimic the events that occur during withdrawal of life support (WLS) in the clinical scenario (66). Male Wister rats (325–395 g) were anesthetized with an intraperitoneal injection of ketamine (80 mg/kg; Cenvet, Australia) and xylazine (10 mg/kg; Provet, Australia), with supplemental doses given as necessary until adequate anaesthesia was achieved. Non-invasive monitoring was established, consisting of measurement of pulse oximetry (Rad-5v, Masimo Inc., Irvine, CA) and continuous electrocardiogram (P55 AC pre-amplifier, Grass Instrument Co., RI). A midline incision was made in the neck of the animal to expose the right carotid artery, which was cannulated for invasive monitoring of arterial pressure via a pressure transducer (Ohmeda, Pty Ltd., Singapore). Once baseline monitoring parameters were recorded, a dose of 500 IU for antemortem heparin was delivered via a side port in the arterial pressure monitoring line. The animal was subjected to WLS via asphyxiation. A fixed warm ischemic time of 10 min followed by a 2-min stand-off period (to mimic Australian federal regulations regarding DCD heart retrieval (34)) was chosen. Upon completion of the stand-off period, the heart and lungs were swiftly excised *en bloc* and immersed in ice-cold Krebs-Henseleit buffer. The aorta and left atrium were fashioned for instrumentation on an *ex-vivo* Langendorff perfusion apparatus. Once the aorta was cannulated onto the *ex-vivo* circuit, the pulmonary veins were rapidly ligated, and the preservation flush (containing Celsior solution (2–3°C) ± supplements) was commenced via the aortic cannula at a flow rate of 15–20 mL/min up to a total volume of 100 mL. The following concentrations of supplements were used: Hi1a: 10 nM; GTN: 100 mg/L; EPO: 5 U/mL; zoniporide: 1 µM. Left atriotomy was performed to prevent left ventricle distension and to facilitate cannulation on the *ex-vivo* apparatus for functional assessment during the working phase of the experiment.

Following the preservation flush, Langendorff reperfusion was commenced for a period of 30 min, using oxygenated Krebs-Henseleit buffer (37°C) to allow stabilization and recovery of the heart. As previously described, the apparatus was converted to a working mode via switching the supply of perfusate from the aortic to the left atrial cannula at a hydrostatic pressure of 15 cm H_2O (preload). Functional parameters (AF, CO, PP and HR) were measured continuously, and CF measured at 5-min intervals, during working mode. Left ventricular free-wall samples were collected at the end of the experiment for additional analysis via Western blot (see supplemental methods). To assess cell death throughout reperfusion, coronary effluent samples were collected at 1, 15, and 30 min of working

mode and LDH levels were measured using the TOX 7 assay kit (Sigma-Aldrich). Duplicate 75 μL aliquots were assayed according to the manufacturer's instructions. The resulting absorbance of the tetrazolium product was measured at 492 nm using a 96-well plate reader and expressed as arbitrary units, normalised to coronary flow per minute.

Peptide production. Recombinant Hi1a was produced by expression as a His_6-maltose-binding protein (MBP) fusion protein in the periplasm of *Escherichia coli* as previously described (26), but with optimisation of the expression and purification conditions to improve the yield of Hi1a. Briefly, *E. coli* BL21(DE3) cells were grown at 30°C in Terrific Broth until the optical density at 600 nm reached 2.0−2.5, at which point the temperature was reduced to 17°C and after a 15 min delay expression of the Hi1a fusion protein was induced with 1 mM IPTG. Cells were harvested after a further 21 h growth. PcTx1 and the PcTx1-R27A/V32A analogue were produced in the same manner with minor modifications to the expression protocol. *E. coli* were grown at 37°C for the entire expression period and harvested approximately 4−5 h after induction. Cell pellets were resuspended in 50 mM Tris, 300 mM NaCl, 5% glycerol, 15 mM imidazole (pH 8.3 for Hi1a or pH 8.0 for PcTx1), and the cells were lysed by high-pressure cell disruption (Constant Systems Limited, United Kingdom). The His_6-MBP-peptide fusion proteins were purified from the clarified soluble lysate over a nickel affinity resin. The resin was washed with the same buffer to elute weakly bound proteins before eluting the Hi1a fusion protein with the same buffer containing 300 mM imidazole. Fusion proteins were exchanged into low (< 30 mM) imidazole buffer using an Amicon Ultra-15 centrifugal concentrators (Merck Millipore, Germany) with a 30 kDa molecular weight cut-off in preparation for liberation of Hi1a from the fusion tag using tobacco etch virus (TEV) protease. The fusion proteins were cleaved in redox buffer containing 3 mM reduced glutathione and 0.3 mM oxidised glutathione at pH 8.3 for Hi1a or pH 8.0 for PcTx1, using ~1 mg of TEV protease per 50 mg of fusion protein. For Hi1a the cleavage reaction was allowed to proceed at 4°C over 3−6 days. For the PcTx1 peptides, cleavage was performed at room temperature for a minimum of 16 h. The recombinant peptides each contain a non-native N-terminal serine residue, which is a vestige of the TEV protease recognition site. The released peptides were purified from the cleavage reaction solutions using reversed-phase high-performance liquid chromatography. The mass of the purified peptides were confirmed using electrospray-ionisation mass spectrometry and pure peptides were lyophilised prior to confirmation of ASIC1a inhibitory activity using two electrode voltage clamp electrophysiology, as described previously for both Hi1a (26) and PcTx1 (24, 67, 68). Unless otherwise noted, lyophilized stocks of peptide were reconstituted in sterile deionised water prior to use.

Generation of cardiomyocytes from human induced pluripotent stem cells. Cardiomyocytes generated in this study were derived from the WTC-11 hiPSC line (Gladstone Institute of Cardiovascular Disease, UCSF) (69, 70). Undifferentiated hiPSCs were maintained on Vitronectin XF (5 µg/mL, Stem Cell Technologies) coated tissue culture dishes as per manufacturer recommendation with either mTeSR medium with supplementation or mTeSR PLUS medium with supplementation (Stem Cell Technologies). Contractile cardiomyocytes were differentiated using a high-density monolayer format as previously described (43). On day 1 of differentiation, hiPSCs were dissociated with 0.5 mM EDTA solution supplemented with 1.1 mM D-glucose. Single-cell suspensions were plated at a density of 1.2×10^5 cells/cm^2 and cultured overnight in mTeSR medium supplemented with 10 µM Y-27632 dihydrochloride (Stem Cell Technologies). Once the monolayer reached approximately 80% confluence (usually the following day), differentiation was induced (day 0). The cells were quickly washed with phosphate-buffered saline (PBS) followed by a change in medium to RPMI (ThermoFisher) containing 3 µM CHIR99021 (Stem Cell Technologies), 500 µg/mL BSA (Sigma Aldrich), and 213 µg/mL ascorbic acid (Sigma Aldrich). After 3 days of culture, the medium was exchanged to RPMI containing 500 µg/mL BSA, 213 µg/mL ascorbic acid, and 5 µM Xav-939 (Stem Cell Technologies). On day 5, the medium was replaced with RPMI containing BSA and ascorbic acid as on day 3. Starting on day 7, the cells were fed every other day with RPMI containing B27 supplement with insulin (Life Technologies). Spontaneous beating was typically observed between days 9 and 11 of differentiation.

In vitro *ischemia-acidosis injury model with hiPSC-CMs*. Differentiated cardiomyocytes were replated on either day 15 or day 17 of differentiation for *in vitro* ischemia/acidosis assays. At the time of replating, a subset of cells (~500,000) was set aside for flow cytometry analysis of cardiomyocyte purity (see supplemental methods). For all experiments, only cell preparations with > 80% sarcomeric α-actinin-positive cardiomyocytes were used. After re-plating, cells were maintained for an additional 7 days in RPMI + B27. To prepare media for ischemia/acidosis injury, 10× HBSS without sodium bicarbonate (Sigma) was diluted to 1× concentration in sterile tissue culture-grade water. Solutions were buffered with either 12 mM HEPES (for pH 7.4 media, Sigma Aldrich) or 12 mM MES (for pH < 6.5, Sigma Aldrich) and the pH adjusted accordingly with 1 M NaOH. The medium was sterile filtered with 0.22 µm syringe filters (Millipore). Unless otherwise noted, the replated cells were treated overnight (18 h) in HBSS with or without peptide under either normoxic (~18.5% O_2; 5% CO_2) or hypoxic (0.5% O_2; 5% CO_2) culture conditions. For reperfusion experiments, the medium was replaced with HBSS pH 7.4 (with or without peptide) after overnight incubation and cells were cultured for 1 h

16

under normoxic conditions. To assess cell death, supernatant was collected and LDH levels were measured using a cytotoxicity detection kit (Roche). For all cell culture experiments, percent cell death was calculated using low and high controls. For low control (LC), cardiomyocytes were cultured overnight in standard culture media (RPMI + B27). For high control (HC), cells were cultured in RPMI + B27 containing 1% Triton X-100 (Sigma-Aldrich).

hiPSC-CM calcium analysis. Cardiomyocytes were replated (2×10^4 per well) in 384-well plates (CellBIND black with clear bottom, Corning) and cultured for 7 days in RPMI + B27. On the day of the experiment, the cells were loaded for 1.5 h at 37°C with FLIPR calcium 4 dye (Molecular Devices) diluted in HBSS pH 7.4. After loading, the plate was transferred to a FLIPR Tetra fluorescent plate reader (Molecular Devices). Calcium transients were measured with excitation wavelengths at 470–495 nm and emission at 515–575 nm. For each plate, the camera gain and intensity were adjusted to optimize signal intensity. Data for each well were expressed as normalized arbitrary fluorescence units. All data were acquired at 0.5 s per read, with baseline measurements for 45 s followed by at least 100 s of data collection after each peptide addition. Concentrated peptide dilutions (in HBSS pH 7.4) were added to each well to give a final concentration of 1 nM, 10 nM, 100 nM, or 1 µM. Calcium amplitude, maximum calcium, minimum calcium, and spontaneous beating rate were analysed using ScreenWorks software (Molecular Devices) and normalized to baseline measurements.

Analysis of ASIC1 from GWAS studies of relevant conditions. To assess whether genetic variation of *ASIC1* associates with cardiovascular disease and stroke, we performed a gene-based level test on GWAS summary data using fastBAT (42) implemented in the Complex-Traits Genetics Virtual Lab (CTG-VL) (71). GWAS summary data contains the statistical information of the association of all genetic variants included in a GWAS against a particular trait. fastBat tests the aggregated effects of a set of genetic variants within or close to ($\pm$ 50 kb) each tested gene (*ACCN1* in this case) using a set-based association approach that accounts for the correlation between genetic variants (i.e. linkage disequilibrium). This provides a more powerful approach over single-variant tests done in GWAS. Specifically, we performed analyses using GWAS summary data for acute MI (N_{cases} =5,948, $N_{controls}$ = 354,176), major coronary heart disease (N_{cases} = 10,157, $N_{controls}$ = 351,037) and MI (N_{cases} = 7,018, $N_{controls}$ = 354,176) from Neale's UK Biobank GWAS database (41) and stroke (including any type of stroke, ischemic stroke, large artery stroke, cardioembolic stroke and small vessel stroke (72) (N_{cases} =40,585, $N_{controls}$ = 406,111).

17

Computational analysis of human translatome data. Transcriptional (mRNA-seq) and translational (Ribo-seq) raw data of human heart were obtained from the Hubner Lab website (http://shiny.mdc-berlin.de/cardiac-translatome/) (39). Quality control checks for both RNA-seq and Ribo-seq data sets were performed to ensure reasonable quality for downstream analysis. Genes that were expressed in >99% of samples were retained. After quality control, 47,094 and 43,183 genes were retained in the RNA-seq and Ribo-seq datasets, respectively. DESeq2 normalization was applied to normalize sequencing depth and RNA composition. The detailed normalization workflow performed by DESeq2 (73) involved four steps. First, the row-wise geometric mean (pseudo-reference sample) is calculated by taking the square root of the product of all expression values across samples for each gene. Second, the ratio of each sample to the row-wise geometric mean was calculating by dividing the expression value of every gene by their row-wise geometric mean within a sample. Third, the normalization factor was calculated for each sample, which is the median value of all ratios for a sample. Lastly, the normalized count was calculated using the normalization factor, in which each raw count in a sample was divided by the normalization factor of that sample, and this was performed for every gene in every sample. The normalized counts were log-transformed to eliminate the effect of extreme values. A total of 80 samples were analysed, including a dilated cardiomyopathy group (65 samples) and a control group (15 samples). We utilized R package ggplot2 (v3.2.1) (74) with box and violin plot to generate the two conditions in one graph for the genes encoding ASIC1, ASIC2, ASIC3, and ASIC4, in order to visualize the distribution of gene expression within one group and compare expression differences between groups.

Statistical Analysis. All data are presented as mean ± SEM. Statistical analyses were performed with GraphPad Prism and comparisons were made with Student's *t* test, one-way analysis of variance (ANOVA), or two-way ANOVA. All data were derived from a minimum of three independent experiments with specific information for each experiment detailed in the relevant figure legend. Differences were considered statistically significant when $p < 0.05$.

Acknowledgements

Author Contributions

M.A.R. designed, performed, and analysed the experiments presented in Fig. 1, 2, and 5, Table 1, and Supplemental Fig. S2, S3, and S5, and wrote the manuscript. S.E.S. designed, performed, and analysed the experiments described in Fig. 3 and 4 and wrote the manuscript. N.J.S. produced, purified, and performed QC analyses for peptides used in Fig. 2 – 5 and Supplemental Fig. S3 and S5. L.G., M.H., and J.E.V. helped design, perform, and interpret experiments described in Fig. 3 and 4. M.E.R., W.G.T., J.N.P., J.Y.S., and L.E.S.H. conceived ideas and provided insights towards interpretation of results shown in Fig. 1 and 2. H.S.C. and X.C. helped perform the experiments described in Fig. 5 and Supplemental Fig. S5. M.A.H.A. helped perform the experiments described in Fig. 1 and 2. Y.S. performed computational analysis presented in Supplemental Fig. S4. J.E.H., G.A.Q., and E.R.P. generated data and analysed ASIC isoform expression in the heart in Fig. 1A. G.C.P. performed GWAS analysis and interpretation presented in Table 2. J.F.F. helped conceive the heart transplant studies and provided intellectual and financial support. B.R., R.J.H., S.M., and S.P. generated and validated the ASIC1a knockout mouse strain used for studies presented in Fig. 1 and Supplemental Fig. S1 and S2. G.F.K. conceived of experimental objectives, provided intellectual and financial support, and directly supervised work related to peptide production utilized across all aspects of the study. P.S.M. conceived of experimental objectives, provided intellectual and financial support, and directly supervised work related to heart transplant modelling. N.J.P. conceived of experimental objectives, provided intellectual and financial support, directly supervised work related to mouse IRI, GWAS analysis, human pluripotent stem cell modelling, and oversaw programmatic decisions regarding study design and completion in close collaboration with P.S.M. and G.F.K. All authors contributed to revisions and final preparation of the manuscript.

References

1. G. Savarese & L.H. Lund, Global public health burden of heart failure. *Card Fail Rev* 3(1), 7-11 (2017).

2. L.E. See Hoe, N. Bartnikowski, M.A. Wells, J.Y. Suen, & J.F. Fraser, Hurdles to cardioprotection in the critically ill. *Int J Mol Sci* 20(15), E3823 (2019).

3. C. Cook, G. Cole, P. Asaria, R. Jabbour, & D.P. Francis, The annual global economic burden of heart failure. *Int J Cardiol* 171(3), 368-376 (2014).

4. J.P. Hellermann, S.J. Jacobsen, B.J. Gersh, R.J. Rodeheffer, G.S. Reeder, & V.L. Roger, Heart failure after myocardial infarction: a review. *Am J Med* 113(4), 324-330 (2002).

5. J. Kobashigawa, A. Zuckermann, P. Macdonald, P. Leprince, F. Esmailian, M. Luu, *et al.*, Report from a consensus conference on primary graft dysfunction after cardiac transplantation. *J Heart Lung Transplant* 33(4), 327-340 (2014).

6. J. Stehlik, L.B. Edwards, A.Y. Kucheryavaya, C. Benden, J.D. Christie, A.I. Dipchand, *et al.*, The registry of the international society for heart and lung transplantation: 29th official adult heart transplant report--2012. *J Heart Lung Transplant* 31(10), 1052-1064 (2012).

7. B.E. Sansbury, A.M. DeMartino, Z. Xie, A.C. Brooks, R.E. Brainard, L.J. Watson, *et al.*, Metabolomic analysis of pressure-overloaded and infarcted mouse hearts. *Circ Heart Fail* 7(4), 634-642 (2014).

8. W.C. Stanley, F.A. Recchia, & G.D. Lopaschuk, Myocardial substrate metabolism in the normal and failing heart. *Physiol Rev* 85(3), 1093-1129 (2005).

9. S.M. Cobbe & P.A. Poole-Wilson, The time of onset and severity of acidosis in myocardial ischaemia. *J Mol Cell Cardiol* 12(8), 745-760 (1980).

10. S.A. Gabel, H.R. Cross, R.E. London, C. Steenbergen, & E. Murphy, Decreased intracellular pH is not due to increased H^+ extrusion in preconditioned rat hearts. *Am J Physiol* 273(5), H2257-H2262 (1997).

11. S. Bhowmick, J.T. Moore, D.L. Kirschner, M.C. Curry, E.G. Westbrook, B.T. Rasley, *et al.*, Acidotoxicity via ASIC1a mediates cell death during oxygen glucose deprivation and abolishes excitotoxicity. *ACS Chem Neurosci* 8(6), 1204-1212 (2017).

12. D.J. Conklin, Y. Guo, M.A. Nystoriak, G. Jagatheesan, D. Obal, P.J. Kilfoil, *et al.*, TRPA1 channel contributes to myocardial ischemia-reperfusion injury. *Am J Physiol Heart Circ Physiol* 316(4), H889-H899 (2019).

13. H. El Banani, Changes in intracellular sodium and pH during ischaemia–reperfusion are attenuated by trimetazidine: comparison between low- and zero-flow ischaemia. *Cardiovasc Res* 47(4), 688-696 (2000).

14. S. Vullo & S. Kellenberger, A molecular view of the function and pharmacology of acid-sensing ion channels. *Pharmacol Res*, 104166 (2019).

15. S. Gründer & X. Chen, Structure, function, and pharmacology of acid-sensing ion channels (ASICs): focus on ASIC1a. *Int J Physiol Pathophysiol Pharmacol* 2(2), 73-94 (2010).

16. J.A. Wemmie, R.J. Taugher, & C.J. Kreple, Acid-sensing ion channels in pain and disease. *Nat Rev Neurosci* 14(7), 461-471 (2013).

17. Y.L. Hu, X. Mi, C. Huang, H.F. Wang, J.R. Song, Q. Shu, *et al.*, Multiple H^+ sensors mediate the extracellular acidification-induced $[Ca^{2+}]_i$ elevation in cultured rat ventricular cardiomyocytes. *Sci Rep* 7, 44951 (2017).

18. Z. Li, Z. Meng, J. Lu, F.M. Chen, W.T. Wong, G. Tse, *et al.*, TRPV6 protects ER stress-induced apoptosis via ATF6α-TRPV6-JNK pathway in human embryonic stem cell-derived cardiomyocytes. *J Mol Cell Cardiol* 120, 1-11 (2018).

19. J. Lipski, T.I. Park, D. Li, S.C. Lee, A.J. Trevarton, K.K. Chung, *et al.*, Involvement of TRP-like channels in the acute ischemic response of hippocampal CA1 neurons in brain slices. *Brain Res* 1077(1), 187-199 (2006).

20. E. Babini, M. Paukert, H.S. Geisler, & S. Grunder, Alternative splicing and interaction with di- and polyvalent cations control the dynamic range of acid-sensing ion channel 1 (ASIC1). *J Biol Chem* 277(44), 41597-41603 (2002).

21. M. Li, K. Inoue, D. Branigan, E. Kratzer, J.C. Hansen, J.W. Chen, *et al.*, Acid-sensing ion channels in acidosis-induced injury of human brain neurons. *J Cereb Blood Flow Metab* 30(6), 1247-1260 (2010).

22. D.C. Immke & E.W. McCleskey, Lactate enhances the acid-sensing Na^+ channel on ischemia-sensing neurons. *Nat Neurosci* 4(9), 869-870 (2001).

23. N.J. Allen & D. Attwell, Modulation of ASIC channels in rat cerebellar Purkinje neurons by ischaemia-related signals. *J Physiol* 543(2), 521-529 (2002).

24. C.A. McCarthy, L.D. Rash, I.R. Chassagnon, G.F. King, & R.E. Widdop, PcTx1 affords neuroprotection in a conscious model of stroke in hypertensive rats via selective inhibition of ASIC1a. *Neuropharmacology* 99, 650-657 (2015).

25. Z.G. Xiong, X.M. Zhu, X.P. Chu, M. Minami, J. Hey, W.L. Wei, *et al.*, Neuroprotection in ischemia: blocking calcium-permeable acid-sensing ion channels. *Cell* 118(6), 687-698 (2004).

26. I.R. Chassagnon, C.A. McCarthy, Y.K. Chin, S.S. Pineda, A. Keramidas, M. Mobli, *et al.*, Potent neuroprotection after stroke afforded by a double-knot spider-venom peptide that inhibits acid-sensing ion channel 1a. *Proc. Natl. Acad. Sci. U.S.A.* 114(14), 3750-3755 (2017).

27. M. Qiang, X. Dong, Z. Zha, X.K. Zuo, X.L. Song, L. Zhao, *et al.*, Selection of an ASIC1a-blocking combinatorial antibody that protects cells from ischemic death. *Proc. Natl. Acad. Sci. U.S.A.* 115(32), E7469-E7477 (2018).

28. G.A. Quaife-Ryan, C.B. Sim, M. Ziemann, A. Kaspi, H. Rafehi, M. Ramialison, *et al.*, Multicellular transcriptional analysis of mammalian heart regeneration. *Circulation* 136(12), 1123-1139 (2017).

29. E.L. Bassler, T.J. Ngo-Anh, H.S. Geisler, J.P. Ruppersberg, & S. Grunder, Molecular and functional characterization of acid-sensing ion channel (ASIC) 1b. *J Biol Chem* 276(36), 33782-33787 (2001).

30. L.M. Nielsen, A.E. Olesen, T. Andresen, M. Simren, H. Tornblom, & A.M. Drewes, Efficacy and safety of PPC-5650 on experimental rectal pain in patients with irritable bowel syndrome. *Basic Clin Pharmacol Toxicol* 116(2), 140-145 (2015).

31. Z.G. Zhang, X.L. Zhang, X.Y. Wang, Z.R. Luo, & J.C. Song, Inhibition of acid sensing ion channel by ligustrazine on angina model in rat. *Am J Transl Res* 7(10), 1798-1811 (2015).

32. A. Baron & E. Lingueglia, Pharmacology of acid-sensing ion channels - physiological and therapeutical perspectives. *Neuropharmacology* 94, 19-35 (2015).

33. P. Menasche, J.L. Termignon, F. Pradier, C. Grousset, C. Mouas, G. Alberici, *et al.*, Experimental evaluation of Celsior, a new heart preservation solution. *Eur J Cardiothorac Surg* 8(4), 207-213 (1994).

34. K.K. Dhital, A. Iyer, M. Connellan, H.C. Chew, L. Gao, A. Doyle, *et al.*, Adult heart transplantation with distant procurement and ex-vivo preservation of donor hearts after circulatory death: a case series. *Lancet* 385(9987), 2585-2591 (2015).

35. A. Iyer, L. Gao, A. Doyle, P. Rao, D. Jayewardene, B. Wan, *et al.*, Increasing the tolerance of DCD hearts to warm ischemia by pharmacological postconditioning. *Am J Transplant* 14(8), 1744-1752 (2014).

36. A. Linkermann, J.H. Brasen, M. Darding, M.K. Jin, A.B. Sanz, J.O. Heller, *et al.*, Two independent pathways of regulated necrosis mediate ischemia-reperfusion injury. *Proc. Natl. Acad. Sci. U.S.A.* 110(29), 12024-12029 (2013).

37. H. Zhu & A. Sun, Programmed necrosis in heart disease: Molecular mechanisms and clinical implications. *J Mol Cell Cardiol* 116, 125-134 (2018).

38. Y.Z. Wang, J.J. Wang, Y. Huang, F. Liu, W.Z. Zeng, Y. Li, *et al.*, Tissue acidosis induces neuronal necroptosis via ASIC1a channel independent of its ionic conduction. *Elife* 4, 1-21 (2015).

39. S. van Heesch, F. Witte, V. Schneider-Lunitz, J.F. Schulz, E. Adami, A.B. Faber, *et al.*, The translational landscape of the human heart. *Cell* 178(1), 242-260.e229 (2019).

40. E.A. King, J.W. Davis, & J.F. Degner, Are drug targets with genetic support twice as likely to be approved? Revised estimates of the impact of genetic support for drug mechanisms on the probability of drug approval. *BioRxiv*, 513945 (2019).

41. The UK Biobank GWAS Summary Statistics (2018). <http://www.nealelab.is/uk-biobank>

42. A. Bakshi, Z. Zhu, A.A. Vinkhuyzen, W.D. Hill, A.F. McRae, P.M. Visscher, *et al.*, Fast set-based association analysis using summary data from GWAS identifies novel gene loci for human complex traits. *Sci Rep* 6, 32894 (2016).

43. C.E. Friedman, Q. Nguyen, S.W. Lukowski, A. Helfer, H.S. Chiu, J. Miklas, *et al.*, Single-cell transcriptomic analysis of cardiac differentiation from human PSCs reveals HOPX-dependent cardiomyocyte maturation. *Cell Stem Cell* 23(4), 586-598.e588 (2018).

44. C.J. Bohlen, A.T. Chesler, R. Sharif-Naeini, K.F. Medzihradszky, S. Zhou, D. King, *et al.*, A heteromeric Texas coral snake toxin targets acid-sensing ion channels to produce pain. *Nature* 479(7373), 410-414 (2011).

45.   T. Besson, E. Lingueglia, & M. Salinas, Pharmacological modulation of Acid-Sensing Ion Channels 1a and 3 by amiloride and 2-guanidine-4-methylquinazoline (GMQ). *Neuropharmacology* 125, 429-440 (2017).

46.   X.H. Zhang, T. Saric, N.Z. Mehrjardi, S. Hamad, & M. Morad, Acid-sensitive ion channels are expressed in human induced pluripotent stem cell-derived cardiomyocytes. *Stem Cells Dev* 28(14), 920-932 (2019).

47.   Y. Herrera, C. Katnik, J.D. Rodriguez, A.A. Hall, A. Willing, K.R. Pennypacker*, et al.*, σ-1 receptor modulation of acid-sensing ion channel a (ASIC1a) and ASIC1a-induced $[Ca^{2+}]_i$ influx in rat cortical neurons. *J Pharmacol Exp Ther* 327(2), 491-502 (2008).

48.   Y.Z. Wang, W.Z. Zeng, X. Xiao, Y. Huang, X.L. Song, Z. Yu*, et al.*, Intracellular ASIC1a regulates mitochondrial permeability transition-dependent neuronal death. *Cell Death Differ* 20(10), 1359-1369 (2013).

49.   P.S. Macdonald, Heart transplantation from DCD donors: from the bedside to the bench. *Transplantation* 101(8), 1753-1754 (2017).

50.   A. Iyer, L. Gao, A. Doyle, P. Rao, J.R. Cropper, C. Soto*, et al.*, Normothermic ex vivo perfusion provides superior organ preservation and enables viability assessment of hearts from DCD donors. *Am J Transplant* 15(2), 371-380 (2015).

51.   L. Gao, J. Tsun, L. Sun, J. Kwan, A. Watson, P.S. Macdonald*, et al.*, Critical role of the STAT3 pathway in the cardioprotective efficacy of zoniporide in a model of myocardial preservation - the rat isolated working heart. *Br J Pharmacol* 162(3), 633-647 (2011).

52.   R.M. Mentzer, Jr., R.D. Lasley, A. Jessel, & M. Karmazyn, Intracellular sodium hydrogen exchange inhibition and clinical myocardial protection. *Ann Thorac Surg* 75(2), S700-S708 (2003).

53.   R.M. Mentzer, Jr., C. Bartels, R. Bolli, S. Boyce, G.D. Buckberg, B. Chaitman*, et al.*, Sodium-hydrogen exchange inhibition by cariporide to reduce the risk of ischemic cardiac events in patients undergoing coronary artery bypass grafting: results of the EXPEDITION study. *Ann Thorac Surg* 85(4), 1261-1270 (2008).

54.   D.J. Hausenloy & D.M. Yellon, Ischaemic conditioning and reperfusion injury. *Nat Rev Cardiol* 13(4), 193-209 (2016).

55.   S. Ghanekar, S. Corey, T. Lippert, & C.V. Borlongan, Pathological links between stroke and cardiac arrest. *Chin Neurosurg J* 2(40) (2016).

56.   J.P. Fanning, L.E. See Hoe, M.R. Passmore, A.G. Barnett, N.G. Obonyo, J.E. Millar*, et al.*, Neuron-specific enolase and matrix metalloproteinase 9 signal perioperative silent brain infarction during or after transcatheter aortic valve implantation. *Am J Cardiol* 123(3), 434-439 (2019).

57.   M. Fisher & J.L. Saver, Future directions of acute ischaemic stroke therapy. *Lancet Neurol* 14(7), 758-767 (2015).

58.   L.H. Opie & H. Kowolik, The discovery of captopril: from large animals to small molecules. *Cardiovasc Res* 30(1), 18-25 (1995).

23

59. G.F. King, Venoms as a platform for human drugs: translating toxins into therapeutics. *Expert Opin Biol Ther* 11(11), 1469-1484 (2011).

60. E.N. Hoagland, T.W. Sherwood, K.G. Lee, C.J. Walker, & C.C. Askwith, Identification of a calcium permeable human acid-sensing ion channel 1 transcript variant. *J Biol Chem* 285(53), 41852-41862 (2010).

61. L.E. See Hoe, S.R. Foster, L. Wendt, H.H. Patel, J.P. Headrick, & J.N. Peart, Regulation of the β-adrenergic receptor signaling pathway in sustained ligand-activated preconditioning. *J Pharmacol Exp Ther* 369(1), 37-46 (2019).

62. M.E. Reichelt, L. Willems, B.A. Hack, J.N. Peart, & J.P. Headrick, Cardiac and coronary function in the Langendorff-perfused mouse heart model. *Exp Physiol* 94(1), 54-70 (2009).

63. F. Gao, J. Zhang, F. Wang, X. Xin, & D. Sha, Cyclosporin A-related cerebral venous sinus thrombosis: A case report. *Medicine (Baltimore)* 97(31), e11642 (2018).

64. J. Gao, B. Duan, D.G. Wang, X.H. Deng, G.Y. Zhang, L. Xu, *et al.*, Coupling between NMDA receptor and acid-sensing ion channel contributes to ischemic neuronal death. *Neuron* 48(4), 635-646 (2005).

65. G. Kumarasinghe, L. Gao, M. Hicks, J. Villanueva, A. Doyle, P. Rao, *et al.*, Improved heart function from older donors using pharmacologic conditioning strategies. *J Heart Lung Transplant* 35(5), 636-646 (2016).

66. L. Gao, A. Doyle, J. Villanueva, S. Scheuer, H.C. Chew, M. Hicks, *et al.*, Enhanced functional recovery of the heart donated after circulatory death determination with antemortem heparin. *J Heart Lung Transplant* in press, doi: 10.1016/j.healun.2020.1002.1016 (available online 3 March 2020).

67. N.J. Saez, M. Mobli, M. Bieri, I.R. Chassagnon, A.K. Malde, R. Gamsjaeger, *et al.*, A dynamic pharmacophore drives the interaction between psalmotoxin-1 and the putative drug target acid-sensing ion channel 1a. *Mol Pharmacol* 80(5), 796-808 (2011).

68. N.J. Saez, E. Deplazes, B. Cristofori-Armstrong, I.R. Chassagnon, X. Lin, M. Mobli, *et al.*, Molecular dynamics and functional studies define a hot spot of crystal contacts essential for PcTx1 inhibition of acid-sensing ion channel 1a. *Br J Pharmacol* 172(20), 4985-4995 (2015).

69. Y. Miyaoka, A.H. Chan, L.M. Judge, J. Yoo, M. Huang, T.D. Nguyen, *et al.*, Isolation of single-base genome-edited human iPS cells without antibiotic selection. *Nat Methods* 11(3), 291-293 (2014).

70. F.R. Kreitzer, N. Salomonis, A. Sheehan, M. Huang, J.S. Park, M.J. Spindler, *et al.*, A robust method to derive functional neural crest cells from human pluripotent stem cells. *Am J Stem Cells* 2(2), 119-131 (2013).

71. G. Cuellar-Partida, M. Lundberg, P.F. Kho, S. D'Urso, L.F. Gutierrez-Mondragon, & L.-D. Hwang, Complex-traits genetics virtual lab: a community-driven web platform for post-GWAS analyses. *BioRxiv*, 518027 (2019).

72. R. Malik, G. Chauhan, M. Traylor, M. Sargurupremraj, Y. Okada, A. Mishra, *et al.*, Multiancestry genome-wide association study of 520,000 subjects identifies 32 loci associated with stroke and stroke subtypes. *Nat Genet* 50(4), 524-537 (2018).

73. M.I. Love, W. Huber, & S. Anders, Moderated estimation of fold change and dispersion for RNA-seq data with DESeq2. *Genome Biol* 15(12), 550 (2014).

74. H. Wickham (2016) *ggplot2: Elegant Graphics for Data Analysis* (Springer-Verlag, New York).

75. J. Schindelin, I. Arganda-Carreras, E. Frise, V. Kaynig, M. Longair, T. Pietzsch*, et al.*, Fiji: an open-source platform for biological-image analysis. *Nat Methods* 9(7), 676-682 (2012).

Tables and Figures

Table 1.

Baseline functional parameters for Langendorff-perfused hearts from ASIC1a$^{+/+}$ and ASIC1a$^{-/-}$ mice

Genotype	Heart Rate (bpm)	LVDP (mmHg)	EDP (mmHg)	+dP/dt (mmHg/s)	-dP/dt (mmHg/s)	CF (mL/min/g)
Wildtype (ASIC1a$^{+/+}$)	353 ± 23	105 ± 4	6.8 ± 0.7	3777 ± 139	−2592 ± 144	35 ± 5
KO (ASIC1a$^{-/-}$)	339 ± 17	101 ± 4	5.1 ± 0.7	3647 ± 236	−2702 ± 148	26 ± 3
p-value	*0.67*	*0.54*	*0.13*	*0.66*	*0.64*	*0.25*

All pre-ischemia functional parameters were measured after more than 30 min of stabilization, except for heart rate, which was measured after 15 min of stabilization, prior to ventricular pacing. All values are expressed as mean ± SEM.

Table 2. Association of polymorphisms in *ACCN1* with ischemic conditions. *ACCN1* gene position: chromosome 12, start: 50451419, end: 50477405)

Genotype	No. of SNPs	SNP start	SNP end	χ^2 statistic	Mean p-value
Acute myocardial infarction [1]	75	rs11377593	rs2242507	152.45	1.4E-02
Major coronary heart disease excluding revascularizations [1]	75	rs11377593	rs2242507	199.11	1.8E-03
Myocardial infarction [1]	75	rs11377593	rs2242507	186.59	3.1E-03
Any stroke [2]	61	rs78972052	rs2242507	81.81	1.5E-01
Any ischemic stroke [2]	62	rs78972052	rs2242507	77.28	2.0E-01
Large artery stroke [2]	63	rs78972052	rs2242507	67.30	3.5E-01
Cardioembolic stroke [2]	61	rs78972052	rs2242507	71.63	2.5E-01
Small vessel stroke [2]	64	rs78972052	rs2242507	147.48	3.9E-03

The number of SNPs inside the *ACCN1* locus was used to calculate the χ^2 statistic and p-value. Source data: GWAS results from [1] UK Biobank from Neale Lab (41) or [2] Malik et al. (72).

Fig. 1. Genetic knockout of ASIC1a protects mouse hearts from *ex vivo* IRI. (**A**) mRNA expression (reads per kilobase million, RPKM) analysis of sorted cardiac cell populations from P56 adult mouse hearts (data extracted from Ref. (28)). ASIC2 was not detected. (**B-F**) Langendorff-perfused hearts from ASIC1a KO (ASIC1a$^{-/-}$, *n* = 10) and WT (ASIC1a$^{+/+}$, *n* = 5) mice were subjected to 25 min of global ischemia followed by 45 min of reperfusion. (**B**) LVDP, expressed as % of pre-ischemia baseline. (**C-E**) Functional parameters measured or calculated after 45 min of reperfusion. (**C**) LVDP, percent baseline (p = 0.025). (**D**) EDP, p = 0.013. (**E**) CF, percent baseline (p = 0.049). (**F**) Cell death after 2 min of reperfusion (units/mL of LDH normalized to reperfusion flow rate and heart weight, U/min/g, p = 0.006). For LVDP and CF, baseline values were obtained immediately prior to ischemia. All data are expressed as mean ± SEM. Statistical significance was determined using two-tailed unpaired Student's *t*-test (*p < 0.05; **p < 0.01).
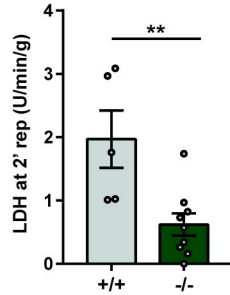
Fig. 2. ASIC1a inhibitors protect isolated mouse hearts from IRI. (**A**) Australian funnel-web spider, *Hadronyche infensa*, from which the ASIC1a inhibitor Hi1a was isolated. (**B**) Schematic of the 3D structure of Hi1a (PDB 2N8F (26)) highlighting the two knottin domains. The 3D structure of PcTx1 (green; PDB 2KNI (67)) is overlaid on the N-terminal knottin domain of Hi1a (blue). The disulfide bonds in each structure are shown as maroon tubes. (**C**) Sequence alignment of Hi1a, PcTx1, and the PcTx1-R27A/V32A analogue. Conserved residues are shown in green, except cysteine residues which are highlighted in maroon. Black circles indicate pharmacophore residues of PcTx1. (**D-H**) Langendorff-perfused hearts from adult (12–14 weeks old) male C57BL/6 mice were subjected to 25 min of global ischemia followed by 45 min of reperfusion. Control hearts (no treatment, *n* = 21) were compared to hearts treated with 10 nM Hi1a (*n* = 7), 10 nM PcTx1 (*n* = 5), 10 nM PcTx1-R27A/V32A, *n* = 11), or 0.1% BSA in water (vehicle control, *n* = 13). For treated hearts, vehicle or peptide solution was infused for 10 min prior to ischemia and during the first 15 min of reperfusion. (**D**) Pre-ischemia LVDP, expressed as % baseline, after exposure to vehicle or peptide for 10 min. (**E**) LVDP over time. (**F-H**) Functional parameters measured or calculated after 45 min of reperfusion including (**F**) LVDP (**G**) EDP and (**H**) CF. For LVDP and CF, baseline values were obtained prior to peptide/vehicle infusion, or 10 min prior to onset of ischemia (no-infusion controls). All data are expressed as mean ± SEM. Statistical significance was determined using one-way ANOVA with multiple comparisons (**p < 0.01, ***p < 0.001).
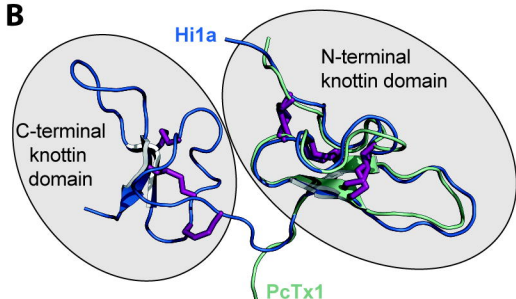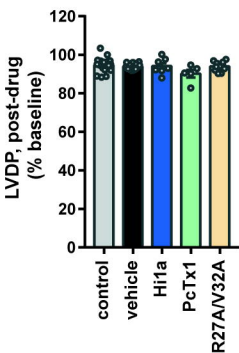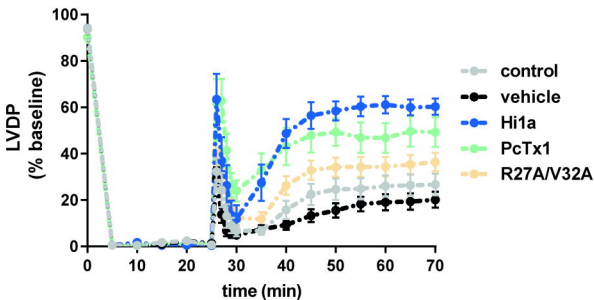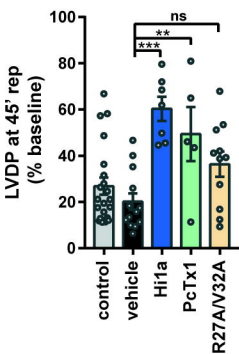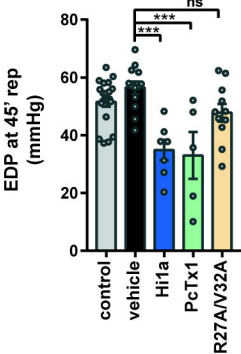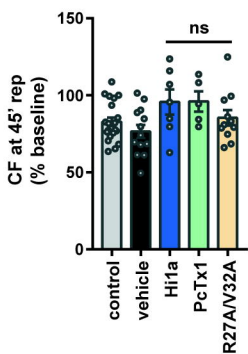
Fig. 3. Hi1a protects isolated rat hearts during long-term hypothermic storage. (**A**) Experimental schematic of 8 h cold storage protocol. (**B-C**) Functional parameters assessed throughout 30 min working mode (post-storage reperfusion) and normalized to pre-storage function. (**B**) Aortic flow (% baseline) over time (left) and after 30 min (right). (**C**) Cardiac output (% baseline) over time (left) and after 30 min (right). All data are expressed as mean ± SEM ($n = 7$ per group). Statistical significance was determined using two-tailed unpaired Student's t-test (*p < 0.05).
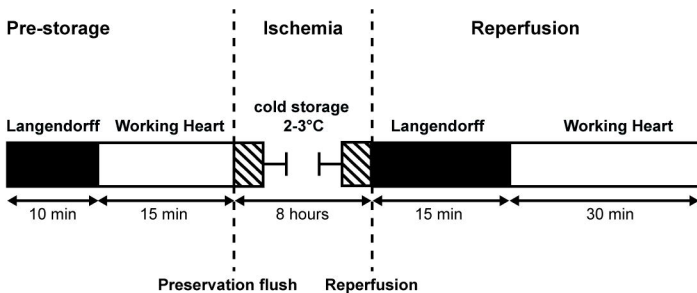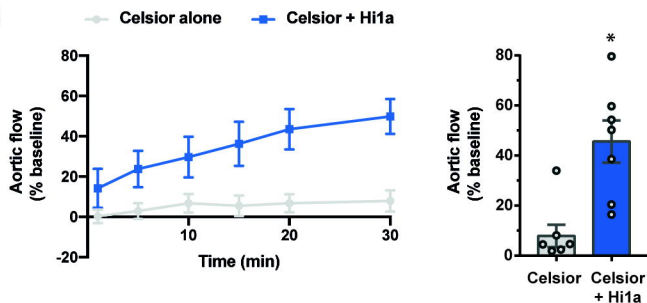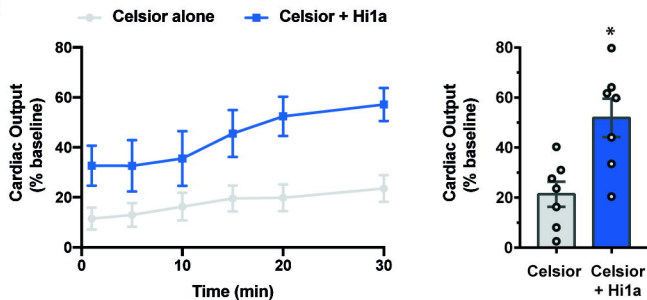
Fig. 4. Hi1a protects rat hearts in a preclinical model of DCD. (**A**) Experimental design to mimic clinical DCD withdrawal. (**B-F**) Biochemical and functional characterisation of DCD hearts flushed with preservation solution (Celsior ± supplementation). (**B**) Arbitrary LDH units in the coronary effluent throughout 30 min working mode (normalized to coronary flow rate, LDH a.u./mL/min). (**C-E**) Assessment of heart function with (**C**) AF (mL/min), (**D**) CO (mL/min), and (**E**) PP (mmHg) plotted over time (left) and after 30 min in working mode (right). (**F**) Representative pRIP3 western blot on pRIP3-IP lysates collected at the end of reperfusion. Molecular masses as determined by BIO-RAD Precision Plus Protein ladder are indicated on the left. Individual lanes represent different hearts ($n = 6$ hearts/group with 3 hearts/group/membrane). (**G**) Quantification of pRIP3 relative signal intensity (upper band, ~46 kDa), normalized internally to Celsior-only control. All data are expressed as mean ± SEM ($n = 6 - 7$/group). For all experimental groups, $n = 6$ hearts. Statistical significance was determined using two-way (panel b) or one-way (panels c-g) ANOVA with multiple comparisons (*p < 0.05; **p < 0.01, ***p < 0.001).

Fig. 5. Hi1a protects hiPSC-CMs from ischemic injury. (**A**) Schematic depicting directed differentiation of hiPSC-CMs (adapted from Ref. (43)). (**B-C**) Analysis of published transcriptomic data (scRNAseq) of cardiac differentiation (43). (**B**) Expression of ASIC1, ASIC2, ASIC3, and ASIC4 at day 0, 2, 5, 15, and 30 of differentiation. (**C**) Gene expression in day-15 hiPSC-CMs. Abbreviations: RYR2 = ryanodine receptor 2; GJA1 = gap junction alpha1 protein (connexin 43). (**D**) Fluorescent imaging of calcium transients (normalized arbitrary fluorescent units (F/F_0)) before and after Hi1a or PcTx1 addition using a FLIPR Tetra system. Representative traces (black dotted line indicates time of peptide addition) and quantification of spontaneous beat rate and calcium amplitude are shown. Amplitude and beat rate are both expressed as a response over baseline (post-addition measurement normalized to pre-addition measurement). (**E**) Cell death (LDH secretion) analysis after overnight treatment in HBSS pH 5.0 with or without Hi1a (top) or PcTx1 (bottom). (**F**) Cell death (LDH) after
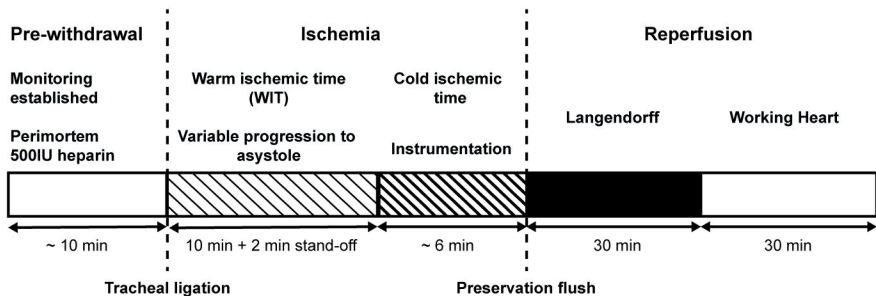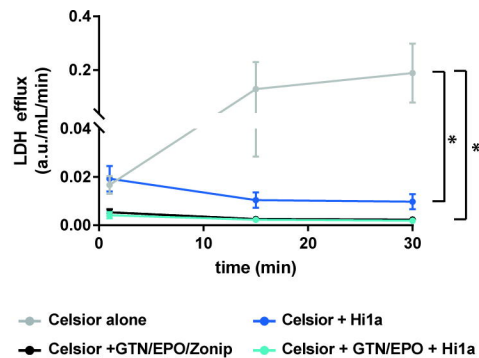
overnight treatment with 20 nM MitTx in HBSS pH 7.4 or HBSS pH 6.0. (**G-H**) Cell death (LDH) after *in vitro* IRI with overnight hypoxic (0.5% O_2) incubation in HBSS pH 5.0 followed by 1 h reperfusion with HBSS pH 7.4 in normoxic conditions. For panels E–H, data are expressed as percent cell death calculated from LDH levels in low (RPMI + B27) and high (1% Triton X-100 in RPMI + B27) controls. All data are expressed as mean ± SEM (n = 3–5 biological replicates with 3–6 technical replicates each). Statistical significance was determined using one-way (panel d-e) or two-way (panel f, g) ANOVA with multiple comparisons (*p < 0.05; **p < 0.01).

Fig. 1

A

B

C

D

E

F

Fig. 2

A

B

Hi1a

C-terminal knottin domain

N-terminal knottin domain

PcTx1

C

```
PcTx1      EDCIPKWKGCVNRHGDCCEGLECWKRRSFEVCVPKTPTEDCIPKWKGCVNRHGDCCEGLECWKRRRSFE-VCVPKTPT
R27A/V32A  EDCIPKWKGCVNRHGDCCEGLECWKRARSFEACVPKTPT
Hi1a       NECIRKWLSCVDRKNCCEGLECYKRRHSFEVCVPIPG--FCLVKWKQCDGRERDCCGLECWKRSGNKSSVCAPIT
           1        10        20        30          40        50        60        70
```

| ←———— *N-terminal PcTx1-like knottin domain* ————→ | ←———— *C-terminal PcTx1-like ICK domain* ————→ |

D

LVDP, post-drug (% baseline)

control vehicle Hi1a PcTx1 R27A/V32A

E

LVDP (% baseline)

time (min)

- - control
- - vehicle
- - Hi1a
- - PcTx1
- - R27A/V32A

F

LVDP at 45' rep (% baseline)

ns

***

**

control vehicle Hi1a PcTx1 R27A/V32A

G

EDP at 45' rep (mmHg)

ns

***

***

control vehicle Hi1a PcTx1 R27A/V32A

H

CF at 45' rep (% baseline)

ns

control vehicle Hi1a PcTx1 R27A/V32A

Fig. 3

A

B

C

Fig. 4

A

Pre-withdrawal	Ischemia		Reperfusion	
Monitoring established	Warm ischemic time (WIT)	Cold ischemic time	Langendorff	Working Heart
Perimortem 500IU heparin	Variable progression to asystole	Instrumentation		

~ 10 min | 10 min + 2 min stand-off | ~ 6 min | 30 min | 30 min

Tracheal ligation

Preservation flush

Legend:
- Celsior alone
- Celsior +GTN/EPO/Zonip
- Celsior + Hi1a
- Celsior + GTN/EPO + Hi1a

Fig. 5